

Supporting Information for

NMR Crystallography of a Carbanionic Intermediate in Tryptophan Synthase: Chemical Structure, Tautomerization, and Reaction Specificity

Bethany G. Caulkins,^{1,**} Robert P. Young,^{1,**} Ryan A. Kudla,¹ Chen Yang,¹ Thomas J. Bittbauer,¹ Baback Bastin,¹ Eduardo Hilario,² Li Fan,² Michael J. Marsella,¹ Michael F. Dunn,² and Leonard J. Mueller^{*,1}

Departments of ¹Chemistry and ²Biochemistry, University of California, Riverside, 92521

** co-first authors

Table of Contents

<i>Figure S1: Variable-Temperature ¹⁵N SSNMR Spectrum of the 2AP Quinonoid Intermediate</i>	S2
<i>Barrier to Proton Exchange</i>	S3
<i>Figure S2: ¹⁵N SSNMR Spectrum of the 2AP Quinonoid Intermediate at 2 kHz MAS</i>	S4
<i>Figure S3: 2D ¹⁵N-¹³C Spectrum of Intermediate prepared with ¹⁵N 2AP and 3-¹³C-Ser</i>	S5
<i>Figure S4: 2D ¹³C CTUC COSY Spectrum of Intermediate prepared with U-¹³C₃; ¹⁵N-Ser</i>	S6
<i>Figure S5: ¹³C SSNMR Spectrum of the 2AP Quinonoid Intermediate at 2 kHz MAS</i>	S7
<i>2AP Quinonoid Candidate Structures</i>	S8
<i>Scheme S1: 2AP Quinonoid Candidate Structures</i>	S9
<i>Table S1: Key Chemical Shifts for 2AP Candidate Structures</i>	S10
<i>The Indoline Quinonoid Intermediate</i>	S11
<i>Figure S6: ¹⁵N SSNMR spectrum of the indoline quinonoid intermediate formed with 2,2',3-¹³C, ¹⁵N-labeled PLP</i>	S12
<i>Figure S7: ¹⁵N SSNMR spectrum of the indoline quinonoid intermediate formed with 2,2',3-¹³C, ¹⁵N-labeled PLP</i>	S13
<i>NMR Crystallography of the Indoline Quinonoid Intermediate</i>	S14
<i>In Silico βS377A Mutant Chemical Shifts</i>	S17
<i>Synthesis of ¹⁵N-2AP</i>	S18
<i>References</i>	S19

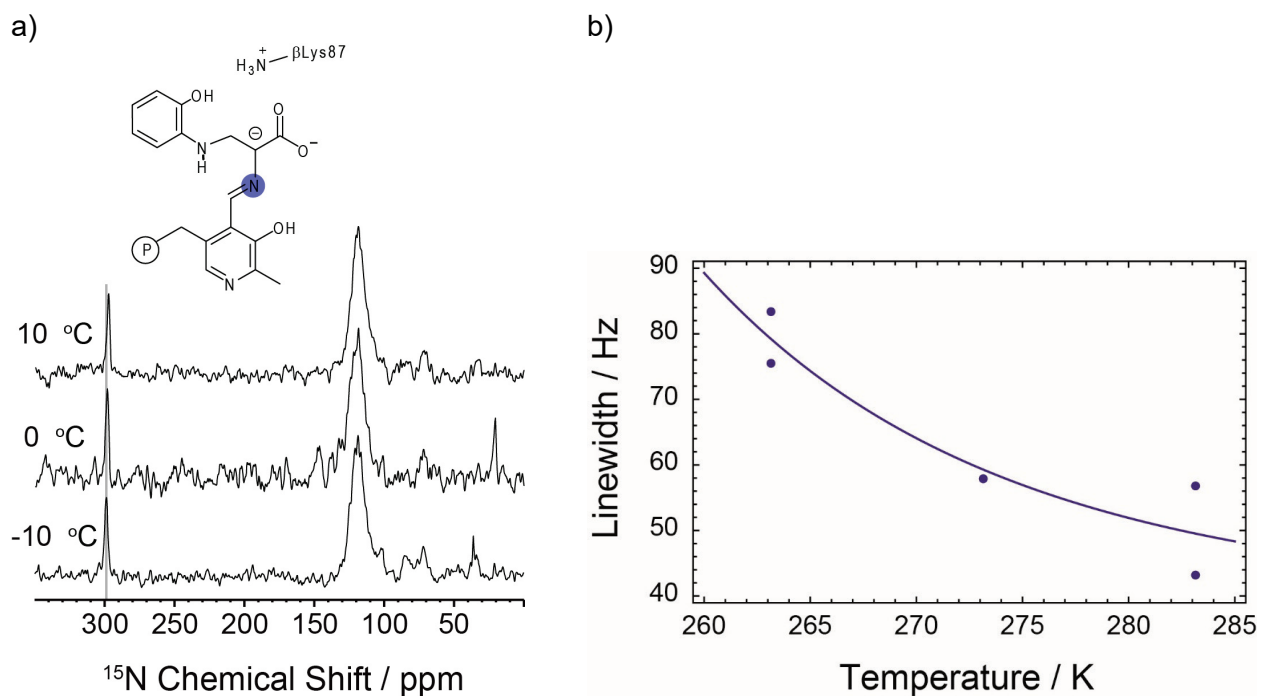


Figure S1: (a) Variable-temperature ^{15}N SSNMR spectra of the reaction of tryptophan synthase microcrystals and ^{15}N -Ser and 2AP to form the 2AP quinonoid intermediate. Experiments were performed at 9.4 T (400.37 MHz ^1H , 40.57 MHz ^{15}N) on a Bruker AVIII spectrometer equipped with an ^1H - ^{15}N triple resonance 4 mm MAS probe, spinning at a MAS rate of 8 kHz, and with the bearing gas cooled to give effective sample temperatures of -10°C , 0°C , and $+10^\circ\text{C}$. Cross-polarization was accomplished at a ^1H spin-lock field of 45 kHz and ^{15}N spin-lock of 37 kHz (ramped ± 2 kHz); 85 kHz Spinal64 ^1H decoupling⁴ was used throughout. Each spectrum consists of the sum of 81,920 transients acquired with a relaxation delay of 4 s, for a total acquisition time of 3 d 19 h. (b) The experimental Schiff-base nitrogen linewidth vs temperature for the 2AP quinonoid. A fit of this data to the two-site fast-exchange model described below allows a barrier to proton exchange of +8.9 kcal/mol to be estimated.

Barrier to Proton Exchange:

The temperature-dependent linewidth of the Schiff-base nitrogen was fit to the two-site exchange model developed by Tian et al.⁶ for the residual linewidth (in Hz) in the fast-exchange limit:

$$\Delta\nu_{1/2} = \frac{1}{\pi T_2} + \frac{4\pi K^2 (v_{\text{phen}} - v_{\text{PSB}})^2}{(1+K)^3 k_f}.$$

In this expression, $1/T_2$ is the spin-spin relaxation rate, v_{phen} and v_{PSB} are the limiting chemical shifts (in Hz) of the Schiff-base nitrogen in the phenolic and protonated Schiff base tautomeric forms, K is the equilibrium constant for the exchange, and k_f is the forward exchange rate (phen to PSB). The exchange rate can be related to the free energy of activation by Eyring's equation,

$$k_f = \frac{K_b T}{h} e^{-\Delta G^\ddagger / RT},$$

where K_b is Boltzmann's constant, h is Plank's constant, and R is the gas constant, to give

$$\Delta\nu_{1/2} = \frac{1}{\pi T_2} + \frac{4\pi K^2 (v_{\text{phen}} - v_{\text{PSB}})^2}{(1+K)^3} \frac{h}{K_b T} e^{\Delta G^\ddagger / RT}.$$

To fit the data, v_{phen} and v_{PSB} were set to their theoretical values of 320.5 ppm and 202.0 ppm (and converted to Hz) and K to the experimentally measured value of 0.23. The best fit to the data in Figure 1b gives the free energy of activation as 8.9 kcal/mol and a limiting linewidth in the fast-exchange limit of 36 Hz ($T_2=8.7$ ms).

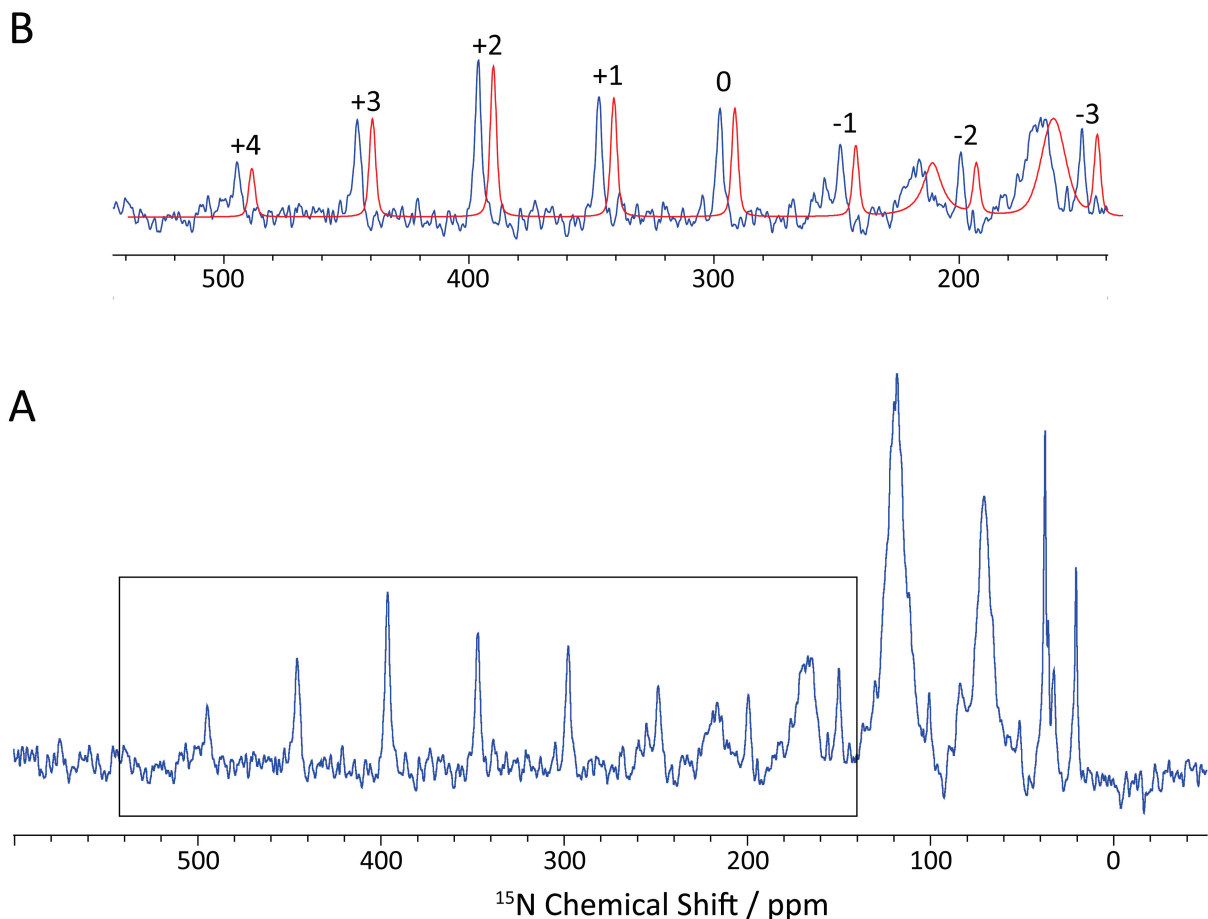


Figure S2: (A) ^{15}N SSNMR spectrum of the reaction of tryptophan synthase microcrystals and ^{15}N -Ser and 2AP to form the 2AP quinonoid intermediate. Experiments were performed at 9.4 T (400.37 MHz ^1H , 40.57 MHz ^{15}N) on a Bruker AVIII spectrometer equipped with an ^1H - ^{15}N triple resonance 4 mm MAS probe, spinning at a MAS rate of 2 kHz, and with the bearing gas cooled to -10°C , giving an effective sample temperature of -5°C . Cross-polarization was accomplished at a ^1H spin-lock field of 45 kHz and ^{15}N spin-lock of 43 kHz (ramped ± 2 kHz); 85 kHz Spinal64 ^1H decoupling⁴ was used throughout. The spectrum consists of the sum of 96,304 transients acquired with a relaxation delay of 4 s, for a total acquisition time of 4 d 13 h. The primary signals arise from the isotropic shifts and spinning sidebands of the Schiff base nitrogen (298.2 ppm) and natural abundance amide backbone nitrogens (122 ppm). (B) A fit (red) to the sideband manifold (blue) for the Schiff base nitrogen performed in Bruker Topspin 3.0 allows for the extraction of the CSA principal axis components $\{\delta_{11}, \delta_{22}, \delta_{33}\} = \{526.8, 368.6, 0.3\}$ ppm. The sideband order is given above each peak.

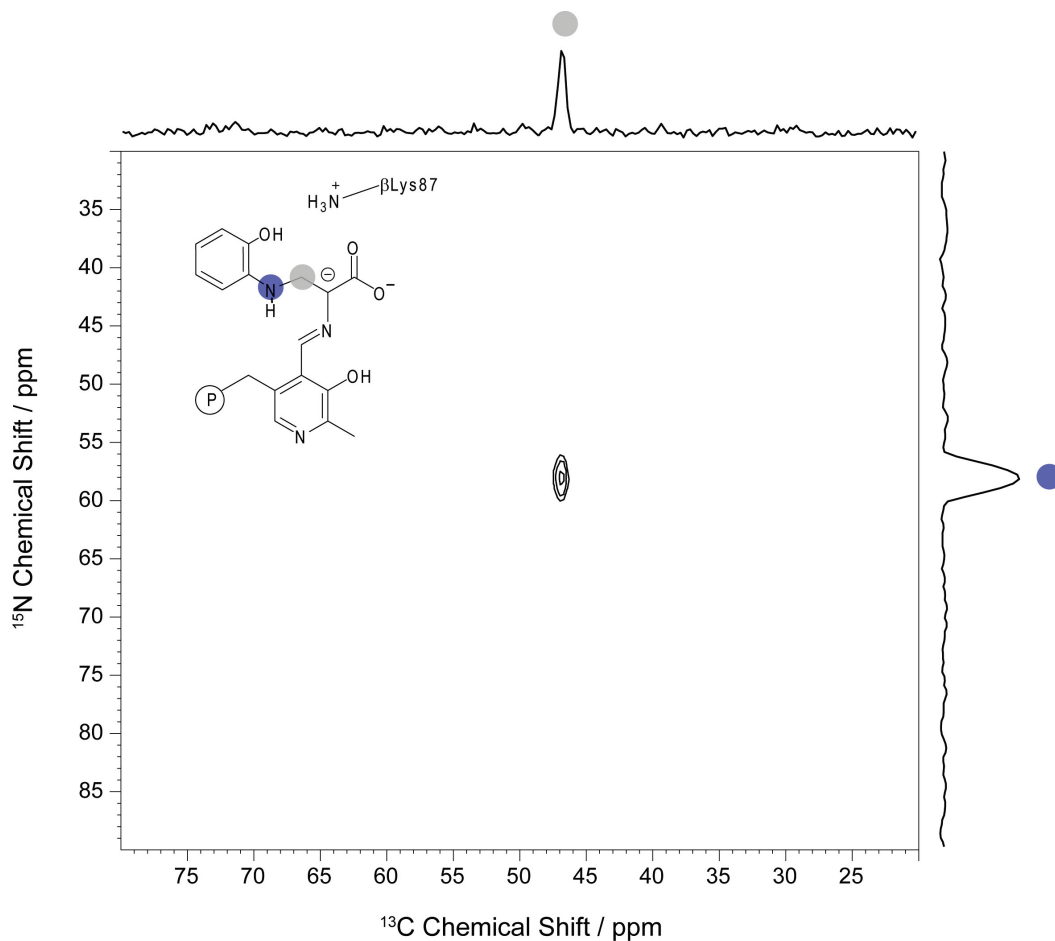


Figure S3: 2D ^{15}N - ^{13}C SPECIFIC CP correlation spectrum³ of the 2AP quinonoid intermediate prepared with 3- ^{13}C -Ser and ^{15}N 2AP, confirming the direct linkage between the 2AP amino group and serine C $^{\beta}$. Experiments were performed at 9.4 T (400.37 MHz ^1H , 100.69 MHz ^{13}C , 40.57 MHz ^{15}N) on a Bruker AVIII spectrometer equipped with an ^1H - ^{13}C - ^{15}N triple resonance 4 mm MAS probe, spinning at a MAS rate of 8 kHz, and with the bearing gas cooled to -15°C , giving an effective sample temperature of -5°C . Initial cross-polarization from ^1H to ^{15}N was accomplished at a ^1H spin-lock field of 45 kHz and ^{15}N spin-lock of 37 kHz (ramped ± 2 kHz); ^{15}N - ^{13}C SPECIFIC CP made use of a ^{15}N spin-lock field of 20 kHz, a ^{13}C spin-lock of 12 kHz (ramped ± 500 Hz), and an 8 ms spin-lock period; 85 kHz Spinal64 ^1H decoupling⁴ was used throughout. Acquisition parameters were as follows: 256 scans were acquired per t_1 increment; 1024 complex points with a dwell of 20 μs (spectral width 50 kHz, total acquisition time 20.48 ms) in t_2 ; 64 complex points with a dwell of 250 μs (spectral width 4 kHz, total acquisition time 8 ms) in t_1 ; recycle delay of 4 s for a total experiment time of 18.6 h. The 2d FID was zero filled to 2048 points in t_2 and 256 points in t_1 and processed with shifted sine bell apodization in both dimensions.

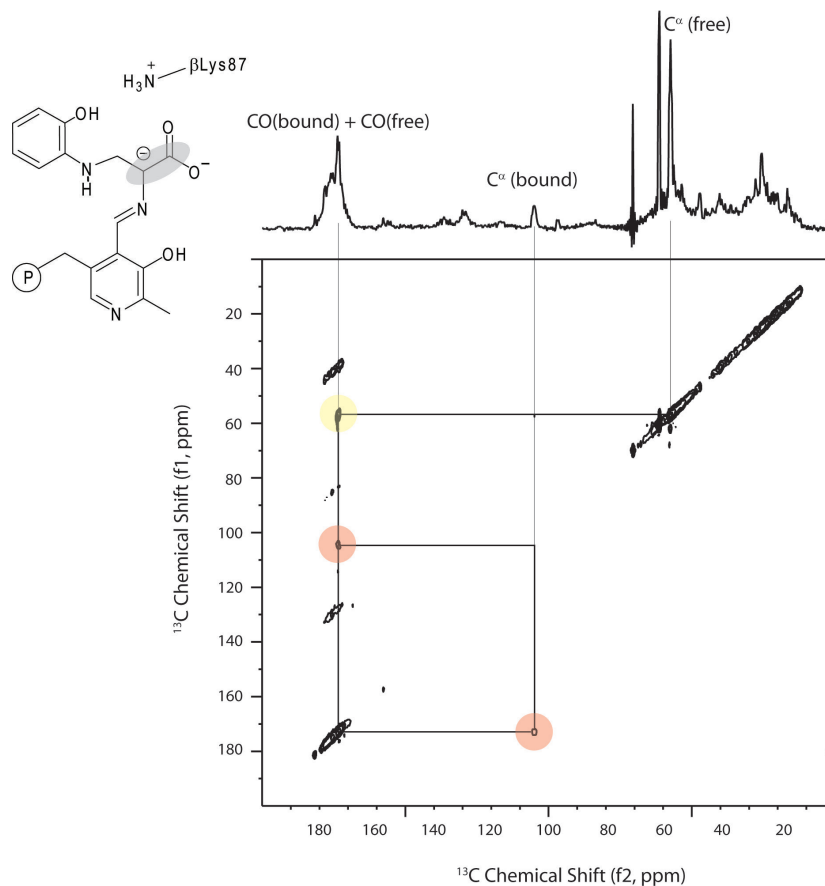


Figure S4: 2D ^{13}C CTUC COSY,² J -based solid-state correlation spectrum of the 2AP quinonoid intermediate prepared with $\text{U-}^{13}\text{C},^{15}\text{N}$ -Ser. Experiments were performed at 9.4 T (400.37 MHz ^1H , 100.69 MHz ^{13}C) on a Bruker AVIII spectrometer equipped with an ^1H - ^{13}C double resonance 4 mm MAS probe, spinning at a MAS rate of 9 kHz, and with the bearing gas cooled to -15°C , giving an effective sample temperature of -5°C . Cross-polarization was accomplished at a ^1H spin-lock field of 45 kHz and ^{13}C spin-lock of 54 kHz (ramped ± 3 kHz); 85 kHz Spinal64 ^1H decoupling⁴ was used throughout. In this experiment, the J -transfer/mixing periods were set to $\tau_1=\tau_2=2.2$ ms; 256 scans were acquired per t_1 increment; 1024 complex points with a dwell of 20 μs (spectral width 50 kHz, total acquisition time 20.48 ms) in t_2 ; 64 complex points with a dwell of 55.56 μs (spectral width 18 kHz, total acquisition time 3.5 ms) in t_1 ; recycle delay of 3 s for a total experiment time of 1 d 4 h. The 2d FID was zero filled to 2048 points in t_2 and 256 points in t_1 and processed with shifted sine bell apodization in both dimensions. The total J -evolution period of 4.4 ms results in a 2D spectrum optimized for CACO cross-peak intensity and allows the observation of the carboxylate shift for the 2AP quinonoid intermediate (red cross peak) even in the presence of a much larger signal from non-specifically bound serine (yellow cross peak) due to the distinct C^α shift of the covalently bound intermediate.

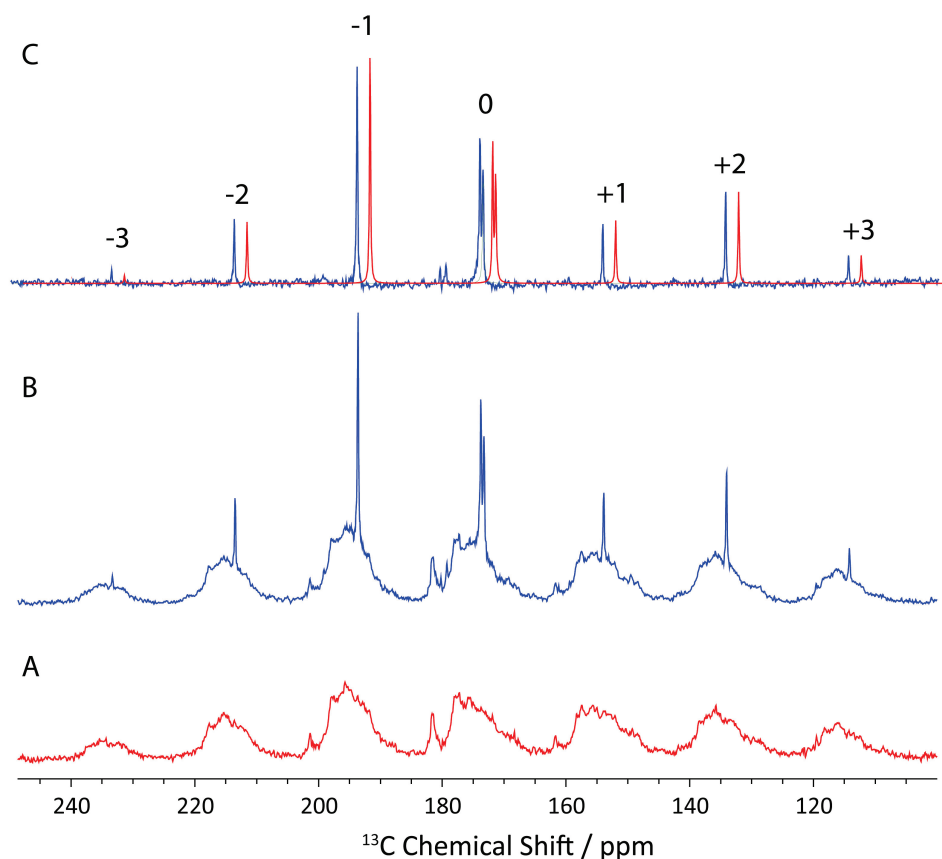
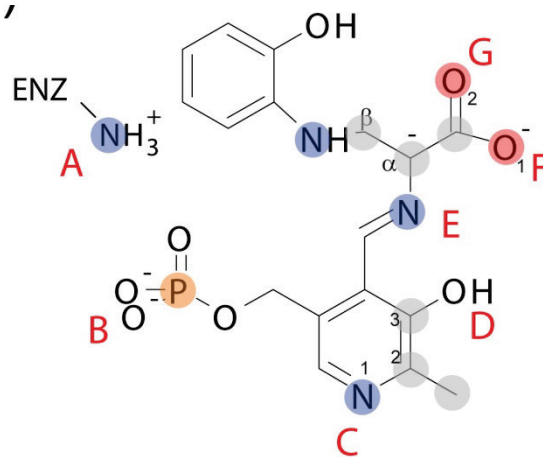


Figure S5: ^{13}C -solid-state NMR cross-polarization magic-angle-spinning (CPMAS) spectra of the reaction of tryptophan synthase microcrystals with (A) L-Ser and 2AP and (B) ^{13}C -Ser and 2AP to form the 2AP quinonoid intermediate. Experiments were performed at 9.4 T (400.37 MHz ^1H , 100.69 MHz ^{13}C) on a Bruker AVIII spectrometer equipped with an ^1H - ^{13}C double resonance 4 mm MAS probe, spinning at a MAS rate of 2 kHz, and with the bearing gas cooled to -10°C , giving an effective sample temperature of -5°C . Cross-polarization was accomplished at a ^1H spin-lock field of 45 kHz and ^{13}C spin-lock of 47 kHz (ramped ± 2 kHz); 85 kHz Spinal64 ^1H decoupling⁴ was used throughout. Each spectrum consists of the sum of 122,880 transients acquired with a relaxation delay of 4 s, for a total acquisition time of 5 d 16 h. The primary signals arise from the isotropic shifts and spinning sidebands of the serine derived carboxylate carbon (173.1 ppm), excess free serine ligand (172.7 ppm and with no detectable sidebands), and natural abundance carbonyl backbone carbons (broad features). (C) The difference between the bottom two spectra gives a spectrum that contains resonances for only the labeled serine derived species. A fit (C, red) to the sideband manifold (C, blue) for the carboxylate carbon performed in Bruker Topspin 3.0 allows for the extraction of the CSA principal axis components, $\{\delta_{11}, \delta_{22}, \delta_{33}\} = \{209.3, 204.7, 105.2\}$ ppm. The sideband order is shown above each peak.

2AP Quinonoid Candidate Structures:

As described in the text, candidate structures with varying protonation states were systematically generated with the goal of introducing as little bias as possible into the pool of candidate structures. Seven ionizable sites were considered on or near the PLP-ligand; these included the ϵ -amino group of β Lys87, the PLP phosphoryl group, the pyridine nitrogen, the pyridoxal oxygen, the Schiff base nitrogen, and both carboxylate oxygen atoms; based on its CSA tensor, the phosphoryl group was taken to be dianionic. Models that had more than a single proton placed at either the pyridoxal oxygen, the Schiff base nitrogen, or the closest carboxylate oxygen, or with a doubly protonated carboxylate were not considered. In total, 30 variations of protonation state were constructed (Scheme S1). These models are labeled using a binary code to indicate whether a site is protonated ("1" – yes, "0" – no) in the following order: (N^ϵ of β Lys87)(phosphoryl group)-(pyridine nitrogen)-(pyridoxyl phenolic oxygen)(Schiff base nitrogen)-(nearer carboxylate oxygen to the Schiff base)(farther carboxylate oxygen); these sites are designated as AB-C-DE-FG. In this nomenclature the species above would be labeled 10-0-10-00. Each model was geometrically optimized and chemical shifts were calculated for comparison with the experimental values (Table S1).



Scheme S1: 2AP Quinonoid Candidate Structures

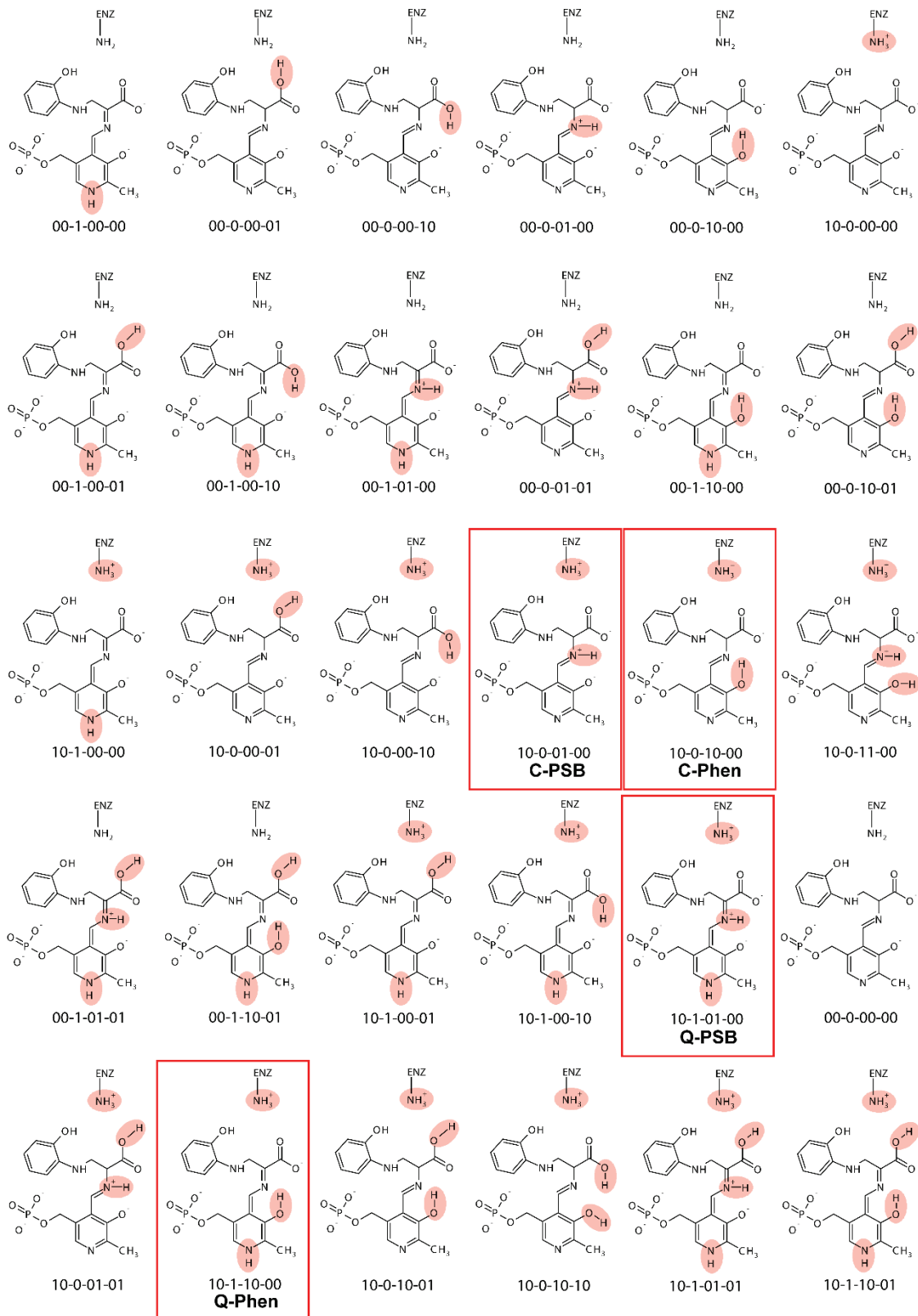
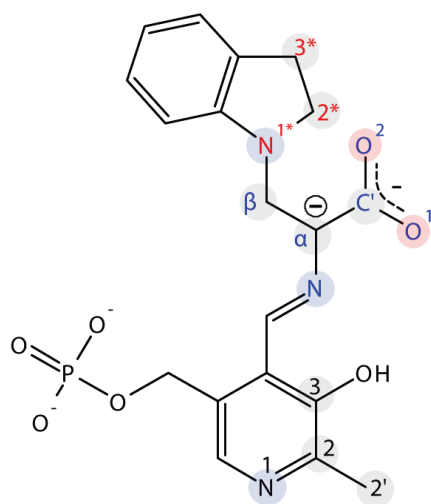


Table S1: Key first-principles chemical shifts (ppm) for the 2AP quinonoid intermediate candidates

Structure	PLP				L-Serine						β K87	2AP	Red. χ^2
	N1	C2	C2'	C3	SB N	C $^\alpha$	C'	C $^\beta$	O1	O2	N $^\epsilon$	N	
10-0-10-00	256.9	141.1	18.7	150.2	320.5	107.9	172.8	47.3	239.6	234.3	26.6	53.8	3.4
00-0-10-00	252.9	136.0	16.8	150.8	325.1	109.6	172.4	46.5	236.4	228.7	12.4	52.9	8.8
10-0-10-01	282.3	144.7	17.0	151.4	310.7	100.6	162.7	45.5	215.0	129.9	26.5	51.3	25.4
00-0-10-01	280.1	144.2	17.9	152.6	312.1	102.2	161.7	48.5	208.4	131.2	18.7	44.2	26.7
10-0-00-00	251.7	144.8	20.8	163.4	369.3	104.1	172.5	46.6	227.9	217.0	26.5	59.7	28.1
10-0-10-10	278.4	140.8	15.6	146.0	329.6	104.8	165.5	43.3	111.4	201.3	27.2	51.0	36.7
00-0-00-00	256.0	144.8	20.8	165.8	376.3	116.0	172.4	45.8	238.3	225.7	21.4	56.5	38.2
10-0-11-00	272.9	139.3	20.0	142.9	212.8	107.0	169.4	44.9	233.5	253.5	27.2	48.7	39.4
10-0-00-01	267.7	150.0	15.3	164.7	334.2	102.7	160.5	46.1	191.0	127.0	28.0	54.1	39.5
10-0-00-10	270.4	149.3	19.7	164.9	302.1	98.4	164.3	44.2	111.4	168.7	27.1	53.5	42.5
00-0-00-01	267.1	148.0	19.5	165.1	340.8	104.1	159.3	47.5	186.1	128.4	17.7	55.2	43.3
00-0-00-10	270.7	147.7	19.9	165.4	306.6	100.2	163.2	43.8	108.4	162.3	15.1	53.3	46.5
00-0-01-00	271.4	145.1	18.7	164.5	204.6	94.5	170.1	46.2	225.8	219.4	12.9	51.1	51.0
10-1-10-01	183.8	134.2	12.7	151.0	320.8	107.8	164.5	44.4	239.7	137.2	26.4	50.3	52.2
10-0-01-00	272.3	149.5	20.6	164.2	202.0	93.2	170.1	47.4	229.9	224.9	26.4	51.9	53.2
00-1-10-01	181.2	132.2	12.3	151.8	320.7	109.8	164.3	47.3	232.7	138.5	29.5	42.7	56.4
10-1-00-10	187.9	139.3	13.6	162.5	322.9	102.6	166.1	42.8	116.9	189.3	27.0	52.3	59.9
10-1-01-00	182.6	136.9	17.0	161.8	209.1	103.2	169.9	45.7	244.0	246.2	26.8	49.9	69.2
00-1-00-10	180.7	137.2	17.7	163.7	330.2	105.9	165.0	44.6	113.0	180.5	13.6	48.0	72.3
10-1-10-00	159.6	127.2	12.9	147.8	321.7	122.8	172.5	45.4	260.5	259.6	26.1	51.5	74.1
10-1-00-01	183.3	140.2	13.0	162.5	365.8	104.9	162.5	43.1	214.9	131.5	26.5	54.4	74.4
00-1-01-00	175.9	133.1	16.1	162.2	211.4	106.2	170.1	46.1	240.7	242.7	15.7	46.9	76.1
00-1-00-01	181.6	137.1	12.4	162.7	367.1	109.6	162.0	46.9	200.1	133.0	26.3	49.3	79.3
00-1-10-00	152.3	124.1	13.0	149.3	318.0	124.8	173.1	46.0	256.7	256.9	14.3	48.3	87.9
10-1-00-00	166.7	129.5	18.5	161.5	384.7	115.3	173.8	43.9	249.5	238.6	25.8	57.8	88.2
00-1-01-01	193.2	141.4	15.9	165.0	199.0	96.4	159.8	46.3	215.2	128.8	17.0	45.0	99.2
10-1-01-01	196.0	143.3	16.9	164.7	193.5	93.6	161.3	44.3	223.2	128.6	27.2	48.6	101.2
00-1-00-00	160.5	127.6	19.5	160.5	387.6	120.6	173.4	44.1	249.0	237.0	28.7	55.2	102.4
00-0-01-01	288.2	152.5	19.7	166.9	186.4	90.4	159.4	45.6	200.1	123.6	14.6	50.0	105.5
10-0-01-01	290.4	152.6	20.0	166.4	184.3	89.5	159.6	45.2	205.9	122.8	27.1	50.0	107.1

The Indoline Quinonoid Intermediate:

As described in the main text, the results for the 2AP quinonoid intermediate, and the protonation state of the pyridine nitrogen in particular, prompted us to reexamine the indoline quinonoid intermediate (Scheme S2) by collecting additional ^{13}C and ^{15}N SSNMR chemical shifts for intermediate formed with labeled PLP (Figures S5 and S6). The PLP ^{13}C and ^{15}N shifts were found to be nearly identical to those for the 2AP quinonoid (Table S2) and a limited computational analysis shows that a 77:23 fast-exchange equilibrium between the carbanionic phenolic and protonated Schiff base tautomers is again the best description of the chemical state (Scheme S3).



Scheme S2. Indoline-quinonoid cofactor-substrate complex ^{15}N , ^{13}C , and ^{17}O enriched sites measured.

Table S2. Experimental Chemical Shifts for the Indoline Quinonoid Intermediate in Tryptophan Synthase

Fragment	Atom	δ_{iso} (ppm)	Ref.
PLP	N1	265.0	a
	C2	145.4	a
	C2'	17.0	a
	C3	154.1	a
	P	4.8	a
L-serine	SB N	296.0	b
	C $^{\alpha}$	103.5	b
	C'	173.0	b
	C $^{\beta}$	54.1	b
	O1	243.0	c
	O2	233.0	c
Indoline	N1*	83.5	b
	C2*	50.5	b
	C3*	28.5	b

Reference (a) this work, (b) Lai. et al¹, and (c), Young et al.⁵

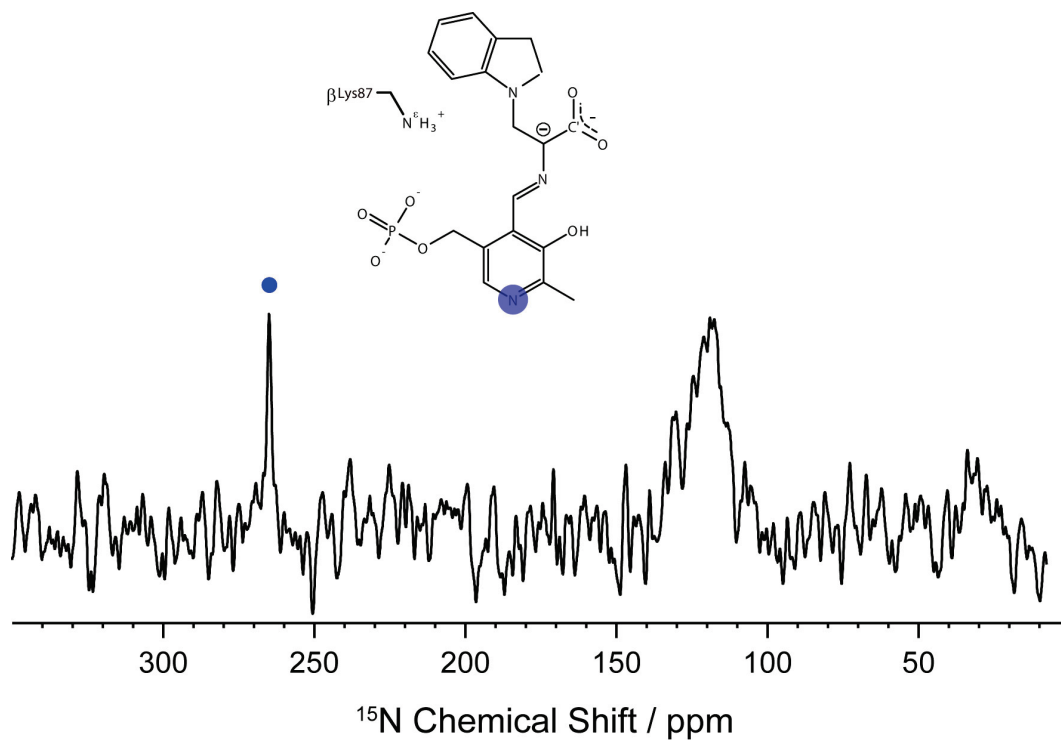


Figure S6: ^{15}N SSNMR spectrum of the indoline quinonoid intermediate formed with 2,2',3- ^{13}C , ^{15}N -labeled PLP tryptophan synthase. Experiments were performed at 9.4 T (400.37 MHz ^1H , 40.57 MHz ^{15}N) on a Bruker AVIII spectrometer equipped with an ^1H - ^{15}N triple resonance 4 mm MAS probe, spinning at a MAS rate of 8 kHz, and with the bearing gas cooled to -15°C , giving an effective sample temperature of -5°C . Cross-polarization was accomplished at a ^1H spin-lock field of 45 kHz and ^{15}N spin-lock of 37 kHz (ramped ± 2 kHz); 85 kHz Spinal64 ^1H decoupling⁴ was used throughout. The spectrum consists of the sum of 16,384 transients acquired with a relaxation delay of 4 s, for a total acquisition time of 17 h. The resonance at 265 ppm can be assigned to the pyridine ring N1 atom and has a chemical shift similar to that in the 2AP quinonoid intermediate (262 ppm).

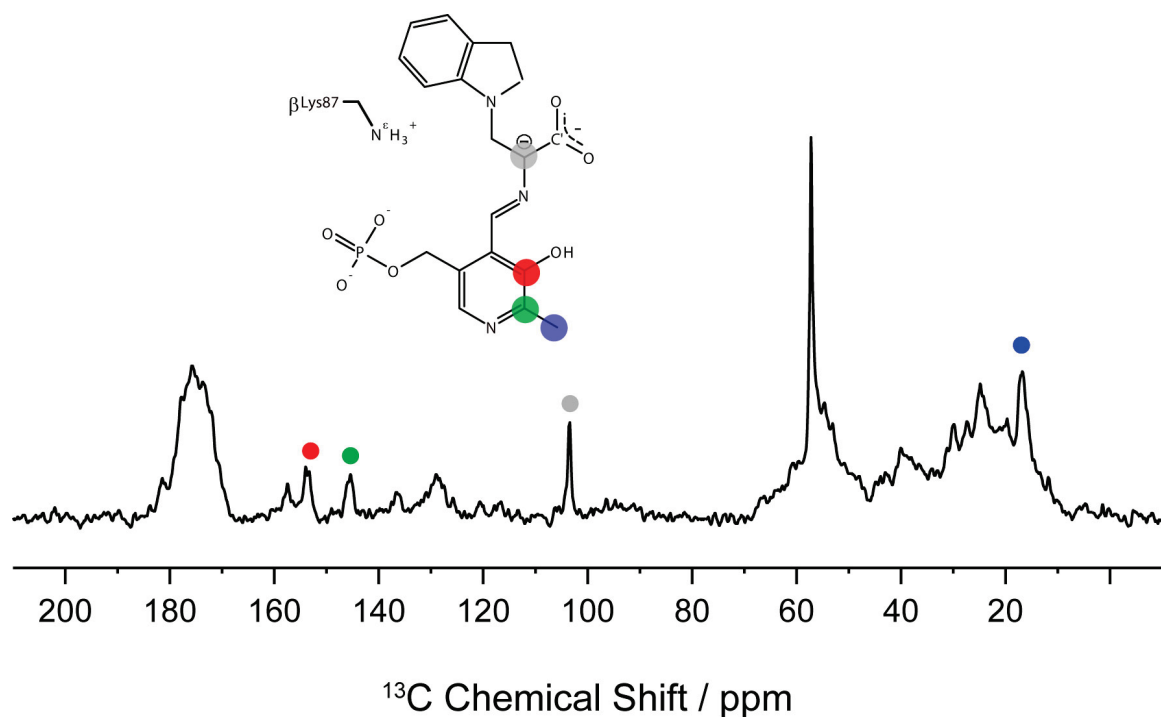
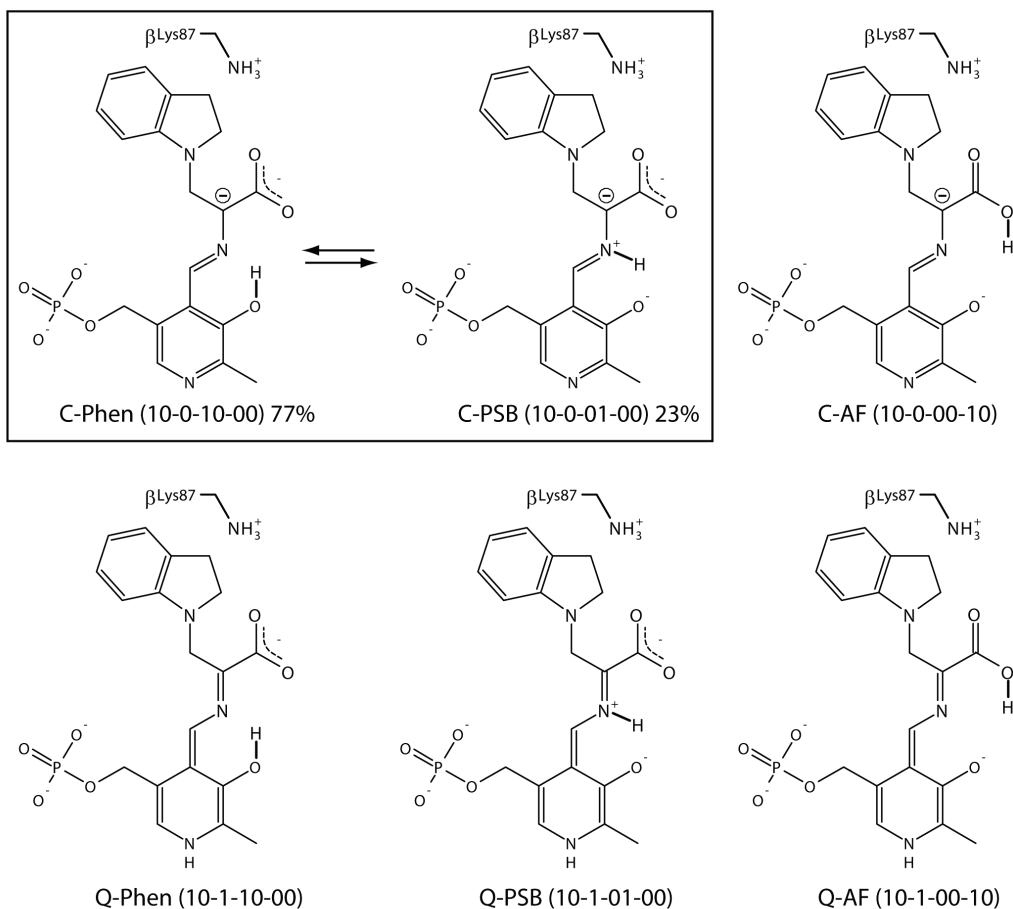


Figure S7: ^{13}C SSNMR spectrum of the indoline quinonoid intermediate formed with 2- ^{13}C -Ser and 2,2',3- ^{13}C , ^{15}N -labeled PLP tryptophan synthase. Experiments were performed at 9.4 T (400.37 MHz ^1H , 100.69 MHz ^{13}C) on a Bruker AVIII spectrometer equipped with an ^1H - ^{13}C triple resonance 4 mm MAS probe, spinning at a MAS rate of 8 kHz, and with the bearing gas cooled to -15°C , giving an effective sample temperature of -5°C . Cross-polarization was accomplished at a ^1H spin-lock field of 45 kHz and ^{13}C spin-lock of 53 kHz (ramped ± 2 kHz); 85 kHz Spinal64 ^1H decoupling⁴ was used throughout. The spectrum consists of the sum of 16,384 transients acquired with a relaxation delay of 4 s, for a total acquisition time of 19 h.

NMR Crystallography of the Indoline Quinonoid Intermediate:

Ab initio calculations: First-principles calculations of the chemical shifts for the $E(Q_3)_{\text{indoline}}$ intermediate were conducted in an analogous manner to that described for the $E(Q_3)_{2AP}$ intermediate in the Experimental section of this article. The 7Å active site cluster was extracted from the X-ray crystal structure PDB ID 3PR2.¹ A limited number of protonation states were tested, (Scheme S3), and these included the C-PSB and C-Phenolic (C-Phen) carbanions, the major tautomers identified for the $E(Q_3)_{2AP}$ intermediate, their corresponding quinonoid forms (protonated pyridine N) Q-PSB, and Q-Phen, and finally C-AF and Q-AF forms representing a carbanion and quinonoid acid form in which the carboxylic oxygen atom nearest the Schiff base nitrogen is protonated.

The chemical shifts predicted for the six candidate structures and their corresponding single site reduced χ^2 values are provided in Table S3. The lowest reduced χ^2 for any single candidate structure was 5.81 corresponding to the C-Phen structure. The best two-site exchange model selected the combination of the C-Phen and C-PSB with populations of 77% and 23% respectively with a reduced χ^2 of 1.17. Table S4 gives the calculated shifts for the C-Phen, C-PSB, the 77:23 C-Phen:C-PSB two-site exchange model, and the experimental chemical shifts. The next best two-site exchange model had a reduced χ^2 of 4.05 placing it well outside the 95% confidence limit.



Scheme S3. The six indoline-quinonoid candidate structures modeled. The best two-site equilibrium selected in the reduced χ^2 fitting procedure is boxed in black and corresponds to populations of 77% and 23% for the C-Phen and C-PSB.

Table S3. Indoline-quinonoid predicted chemical shifts (ppm).

Fragment	Atom	C-Phen	C-PSB	C-AF	Q-Phen	Q-PSB	Q-AF
PLP	N1	261.8	276.3	273.8	151.4	173.5	178.0
	C2	142.3	152.8	155.9	127.6	138.8	143.5
	C2'	18.4	20.3	21.8	16.0	18.3	19.9
	C3	150.2	165.4	166.3	147.8	161.9	162.6
L-serine	SB N	325.5	198.7	298.6	326.2	209.8	327.2
	C ^α	107.3	92.3	100.5	123.7	104.0	102.1
	C'	171.7	168.5	164.2	171.6	168.8	166.4
	C ^β	51.0	51.2	48.1	49.6	49.8	47.6
	O1	254.7	242.4	114.4	278.3	262.5	119.2
	O2	228.2	216.5	161.6	256.4	242.4	186.7
Indoline	N1*	84.8	83.9	86.2	81.1	80.5	83.9
	C2*	50.2	50.0	50.6	50.1	50.2	51.1
	C3*	25.6	25.3	25.0	24.9	24.6	24.9
	Red. χ^2	5.8	51.7	44.2	85.7	70.8	65.3

Table S4. Predicted chemical shifts (ppm) for the C-Phen, C-PSB, the best-fit 2-site 77%:23% C-Phen:C-PSB equilibrium, and corresponding experimental chemical shifts for the indoline-quinonoid intermediate.

Fragment	Atom	C-Phen	C-PSB	2-Site	Exp.
PLP	N1	261.8	276.3	265.2	265.0
	C2	142.3	152.8	144.7	145.4
	C2'	18.4	20.3	18.9	17.0
	C3	150.2	165.4	153.8	154.1
L-serine	SB N	325.5	198.7	295.8	296.0
	C ^α	107.3	92.3	103.8	103.5
	C'	171.7	168.5	170.9	173.0
	C ^β	51.0	51.2	51.1	54.1
	O1	254.7	242.4	251.8	243.0
	O2	228.2	216.5	225.4	233.0
Indoline	N1*	84.8	83.9	84.6	83.5
	C2*	50.2	50.0	50.1	50.5
	C3*	25.6	25.3	25.5	28.5
	Red. χ^2	5.81	51.66	1.17	

NBO Partial Charges

NBO partial charge calculations for the C-Phen, C-PSB, Q-Phen, and Q-PSB candidate structures were conducted in an identical manner as detailed for the 2AP-quinonoid in the main text experimental section. The partial charge values for the key C^α and C4' positions are provided in Table S5. The results indicate that the greatest charge separation between the C^α and C4' having the most negative charge at C^α and most positive value at C4' was predicted for the C-PSB tautomer as was predicted for the 2AP-quinonoid intermediate.

Table S5. Partial atomic charges for the candidate structures

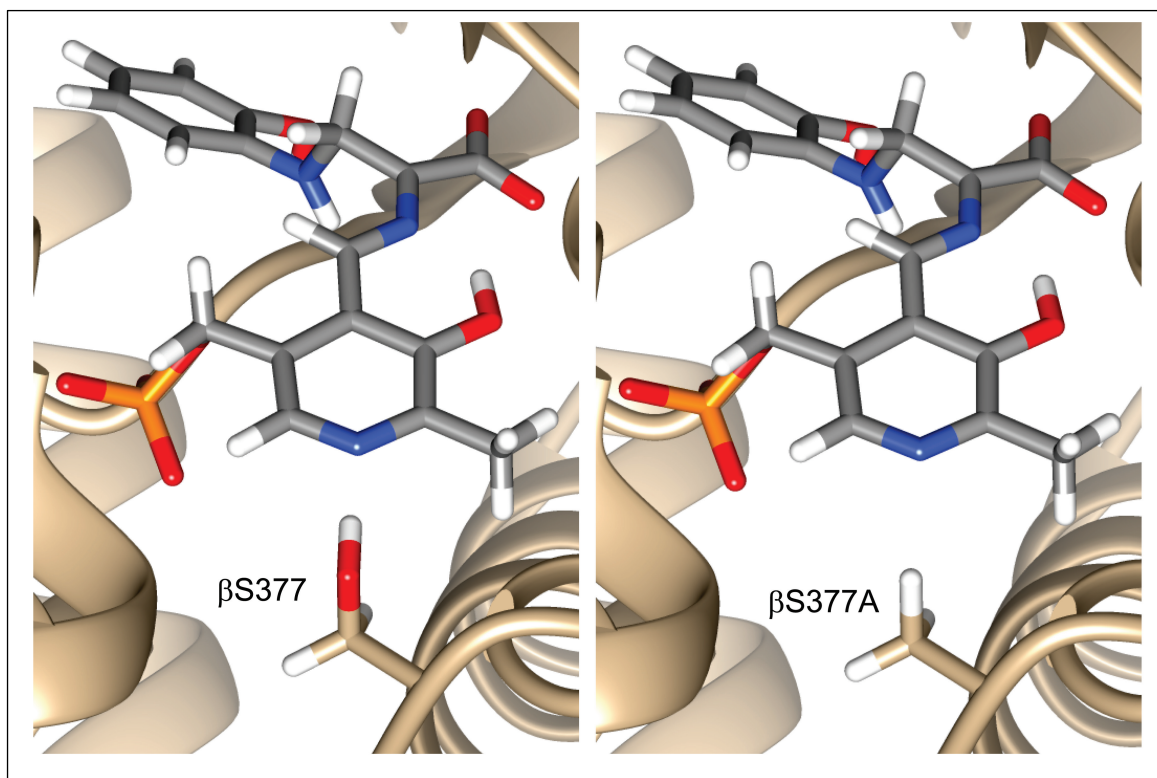
Atom	C-Phen	C-PSB	Q-Phen	Q-PSB
C ^α	-0.090	-0.122	0.012	-0.040
C4'	-0.084	0.015	-0.107	-0.039

In Silico β S377A Mutant Chemical Shifts

The C-Phen β S377A *in silico* mutant was constructed by replacing the β Ser377 hydroxyl group in the C-Phen candidate structure with a single hydrogen atom using GaussView 5.0. No additional optimization was performed prior to calculating the magnetic shielding/shift values using the same protocol as described in the experimental section of the main text.

Table S6: Calculated isotropic chemical shifts (in ppm) for the C-Phen wild type (WT) and *in silico* β S377A mutant.

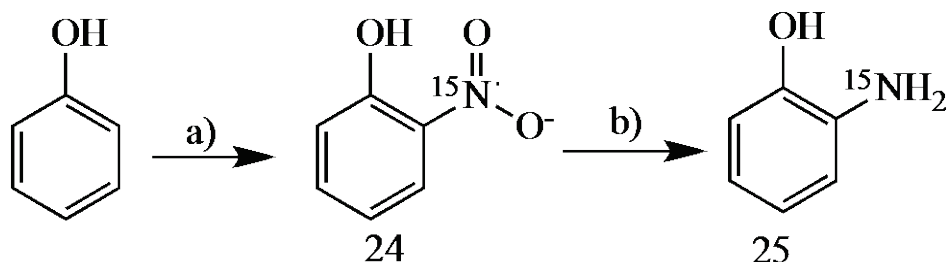
Fragment	Atom	WT	β S377A
PLP	N1	256.9	305.1
	C2	141.1	143.4
	C2'	18.7	20.7
	C3	150.2	149.3
L-Ser	SB N	320.5	317.1
	C α	107.9	105.5
	C'	172.8	172.5
	C β	47.3	47.5
	O1	239.6	234.7
	O2	234.3	228.3
BK87	N ϵ	26.6	26.1
2AP	N	53.8	54.2



Synthesis of ^{15}N -2AP:

2-aminophenol was prepared ^{15}N labeled (^{15}N -2AP) using the following literature protocol.⁷⁻⁸

General. Chemicals and solvents were purchased from Sigma Aldrich and used without further purification. Unless otherwise noted, reactions were performed using standard synthetic organic techniques under an atmosphere of nitrogen gas. Nuclear magnetic resonance (NMR) spectra were acquired using a Varian Inova 300 MHz spectrometer. Chemical shifts (δ) are reported in parts per million (ppm) and are calibrated to the residual solvent peak. Coupling constants (J) are reported in Hz.



Scheme S4: Synthesis of [^{15}N]-2AP a) H^{15}NO_3 (10M), Tetra-*n*-butylammonium bromide (TBAB), Ethylene Dichloride b) 10% Pd/C, NaBH_4

Compound 24: Phenol (0.75 g, 7.8 mmol) was dissolved in ethylene dichloride (16 mL) and stirred at room temperature. To the mixture tetrabutylammonium bromide (0.25 g, 0.78 mmol), ^{15}N -nitric acid (70 wt%, 1 g), and sufficient water to make up the nitric acid concentration to 6 wt %. The reaction was stirred overnight at room temperature. Upon completion of the reaction, the aqueous layer was separated from the organic layer. The aqueous layer was extracted with pentane, combined with the other organic layer, and the combined organic layers was washed once with DI water. A silica plug eluting with 1:3 EtOAc/Hex gave 0.262 g of **24** (24 % yield). ^1H NMR (CDCl_3 , 300 MHz): δ 7.01 (1H, dt, J = 1.5, 5.7 Hz), δ 7.18 (1H, dd, J = 1.5, 7.2 Hz), δ 7.60 (1H, dt, J = 1.5, 5.7 Hz), δ 8.13 (1H, dd, J = 1.5, 6.9 Hz), δ 10.6 (1H, s).

Compound 25: In a flame dried 3 neck flask, affixed with reflux condenser, a positive flow of N_2 , and a balloon 0.076 g of 10 % Pd/C was dissolved in 7.0 mL of DI water. Sodium Borohydride (0.14 g, 3.8 mmol) was then added and the reaction stirred at room temperature. **24** (0.27 g, 1.9 mmol) was dissolved in 2 M NaOH (10 mL) and added dropwise. The reaction was stirred at room temperature until the yellow color disappears and then the reaction mixture was filtered. The filtrate was acidified with 2 M HCl, filtered once again, and then neutralized with 0.5 M NaOH. The product was extracted with diethyl ether, and dried over anhydrous magnesium sulfate. Upon removal of the solvent, 200 mg of **25** was isolated (96 % yield). ^1H NMR (CDCl_3 , 300 MHz) δ 6.66-6.8 (4 H, m) HRMS (m/z): [M^+] calculated for $\text{C}_6\text{H}_8\text{NO}$ 110.0498; found 110.0449.

Supporting Information References:

- (1) Lai, J.; Niks, D.; Wang, Y.; Domratcheva, T.; Barends, T. R.; Schwarz, F.; Olsen, R. A.; Elliott, D. W.; Fatmi, M. Q.; Chang, C. E.; Schlichting, I.; Dunn, M. F.; Mueller, L. J. *J. Am. Chem. Soc.* **2011**, *133*, 4.
- (2) Chen, L. L.; Olsen, R. A.; Elliott, D. W.; Boettcher, J. M.; Zhou, D. H. H.; Rienstra, C. M.; Mueller, L. J. *J. Am. Chem. Soc.* **2006**, *128*, 9992.
- (3) Baldus, M.; Petkova, A. T.; Herzfeld, J.; Griffin, R. G. *Mol. Phys.* **1998**, *95*, 1197.
- (4) Fung, B. M.; Khitrin, A. K.; Ermolaev, K. *J. Magn. Reson.* **2000**, *142*, 97.
- (5) Young, R. P.; Caulkins, B. G.; Borchardt, D.; Bulloch, D. N.; Larive, C. K.; Dunn, M. F.; Mueller, L. J. *Angew. Chem. Int. Ed* **2016**, *55*, 1350.
- (6) Tian, Y.; Kayatta, M.; Shultis, K.; Gonzalez, A.; Mueller, L. J.; Hatcher, M. E. *J. Phys. Chem. B* **2009**, *113*, 2596.
- (7) Joshi, A. V.; Baidoosi, M.; Mukhopadhyay, S.; Sasson, Y. *Org. Process Res. Dev.* **2003**, *7*, 95.
- (8) Smith, C. J.; Ali, A.; Chen, L.; Hammond, M. L.; Anderson, M. S.; Chen, Y.; Eveland, S. S.; Guo, Q.; Hyland, S. A.; Milot, D. P.; Sparrow, C. P.; Wright, S. D.; Sinclair, P. J. *Bioorg. Med. Chem. Lett.* **2010**, *20*, 346.